Three-Phase Reactor Model for Hydrotreating in Pilot Trickle-Bed Reactors

Hans Korsten and Ulrich Hoffmann
Institut für Chemische Verfahrenstechnik, TU Clausthal, Leibnizstr. 17, D-38678 Clausthal-Zellerfeld, Germany

A three-phase reactor model for describing the hydrotreating reactions in a trickle-bed reactor was developed. It includes correlations for determining mass-transfer coefficients, solubility data, and properties of the compounds under process conditions. The model, based on the two-film theory, was tested with regard to the hydrodesulfurization of vacuum gas oil in a new high-pressure pilot plant operated under isothermal conditions. The sulfur content of the product oil was found to depend strongly on the gas/oil flow ratio within the reactor. This is due to the inhibiting effect of hydrogen sulfide on the chemical reaction rates described by Langmuir–Hinshelwood kinetics. The poor conversion which, in contrast to industrial plants, is often observed in pilot plant reactors can be explained by incomplete catalyst wetting produced by low liquid velocities. The simulation shows a good agreement with the experiments carried out in a wide range of temperature, pressure, space velocity and gas/oil ratio.

Introduction

Since it is important to minimize air pollution caused by firing mineral oil products, the deep desulfurization of oil fractions is a central matter of concern to every refinery. To maximize the yield of high-quality products containing a low sulfur content, we must know how the process conditions affect hydrodesulfurization.

For the interpretation of kinetic data and the development of new catalysts experiments have to be carried out in a pilot plant trickle-bed reactor. Since the length of an industrial hydrodesulfurization reactor is normally 10–20 times higher than a pilot-scale reactor, it is not possible to operate both reactors at the same weight hourly space velocity (WHSV) and the same superficial mass flow velocity simultaneously. In most cases the experiments are carried out at industrial space velocity, causing the mass flow in the pilot-scale reactor to be 10–20 times lower. This is accompanied by the lower conversion in the small reactor that has often been observed.

Taking the pseudohomogeneous plug-flow model as a basis for their argumentation, Henry and Gilbert (1973) suggested that this effect is due to a lower liquid holdup in the pilot plant reactor. Mears (1974) based the lower conversion on an incomplete catalyst wetting that is due to the relatively low liquid flow. A reliable scale-up of pilot plant data to an industrial trickle-bed reactor using a modified pseudohomogeneous plug-flow model suffers from the problem that the holdup model and the catalyst wetting model are of the same structure concerning the influence of space velocity and length of the reactor. Thus it is difficult to distinguish which phenomenon causes the lower conversion in small reactors (Paraskos et al., 1975).

The investigation of the hydrodesulfurization of model compounds especially shows a large inhibiting effect of hydrogen sulfide on conversion (Gates et al., 1979; Vrinat, 1983; Parijs and Froment, 1986; Parijs et al., 1986). By using complex hydrocarbon mixtures, Gates et al. (1979), Stephan et al. (1985), and Papayannakos and Marangozis (1984) came to an analogous result. Since the concentration of hydrogen sulfide increases with the reactor length, the pseudohomogeneous plug-flow model cannot yield satisfying results, because a change of the gas-phase concentrations and the mass transfer between the phases are neglected. For a reliable estimation and scale-up of pilot plant data, a three-phase reactor model is necessary.

We present a new simulation method for hydrodesulfurization of vacuum gas oil in trickle-bed reactors. The mass balances are described by a reactor model that is based on the two-film theory (Hofmann, 1977). The procedure includes correlations to estimate mass-transfer coefficients, gas solubilities, and the properties of oils and gases under process

Correspondence concerning this article should be addressed to U. Hoffmann.
Current address of Hans Korsten: Haldor Topsøe A/S, Nymøllevej 55, DK-2800 Lyngby, Denmark.

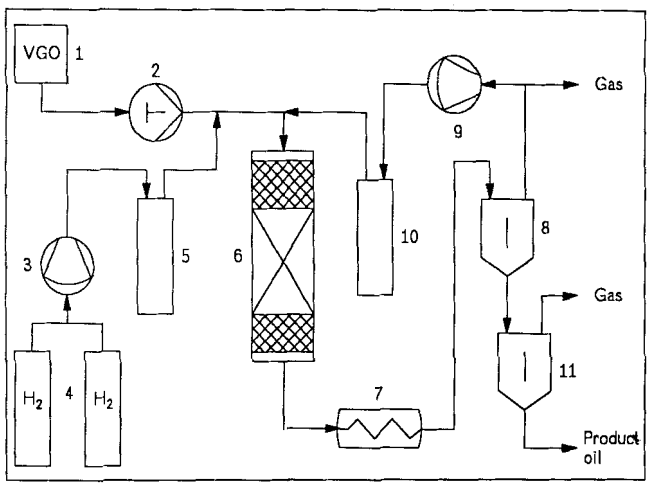

Figure 1. Simplified experimental apparatus.

conditions. The rate of chemical reaction is described by a Langmuir–Hinshelwood formulation. For the experimental verification and parameter estimation, we have constructed a new high-pressure pilot plant (Korsten and Hoffmann, 1995). The residence-time distributions of the gas and of the liquid phase in the trickle-bed reactor show that axial dispersion in both phases can be neglected. It is obvious that the low conversion in pilot plant reactors is due to an incomplete catalyst wetting and can be correlated with the contacting effectiveness recommended by Satterfield (1975).

The model presented in this article is in good agreement with the experimental results where the most important parameters have been changed within a wide range.

Exerimental Equipment and Procedure

For the experimental determination of hydrodesulfurization using catalysts in their original size a new pilot plant reactor system has been constructed, as shown in Figure 1. The liquid reactant in the storage vessel (1) is preheated up to about 100°C to reduce the viscosity of the feed. Then it is metered in the reactor section by means of a high-pressure piston pump (2). The maximum feed rate is about 2,400 cm^3/h. A second unit is the gas supply module. A diaphragm compressor (3) pressurizes the hydrogen contained in the cylinders (4) up to 45 MPa. The following pressure vessel (5) has a function of a shock absorber. This is necessary to guarantee a constant flow because the gas flow generated by the compressor is rich on pulsation. An electronic mass-flow controller installed behind the buffer guarantees a constant flow rate up to 3 Nm^3/h. Now both gas and liquid pass through the trickle-bed reactor (6).

The reactor is designed as a tube with an inside diameter of 3 cm and a length of 125 cm. The length of the reactor is subdivided into three sections. The first section, having a length of 33.5 cm, was packed with inert SiC particles. This entrance section was used to heat up the mixture to a maximum temperature of 500°C, and to provide a uniform distribution of gas and liquid and a hydrogen saturation of the feed. The following section with a length of 66.5 cm contained a packing of 160-g catalyst, and inert particles. The catalysts used were commercial $NiMo/Al_2O_3$ extrudates with a trilobe shape and an equivalent diameter of 1.72 mm. For all the experiments reported here a single charge of the presulfided catalysts was used. The inert exit section was packed with SiC particles of nearly the same size as the catalyst and the particles in the other reactor sections. At the center line of the reactor there is a thermowell containing ten thermocouples used to control the axial temperature profile within the reactor. The reactor temperature was maintained at the desired level by five electric heaters, which provided an isothermal temperature along the active reactor section. The greatest deviation from the desired value was about 1°C.

A water-cooling system (7) is located near the reactor exit to cool down the products to about 50°C. The high-pressure separator (8) is installed to ensure that a liquid-free gas phase can be separated from the system. A back-pressure regulator is located at the gas exit line to ensure a constant reactor pressure. A part of the effluent gas stream can be recycled with a diaphragm compressor (9) via the high-pressure vessel (10) and a second mass-flow controller to adjust the required flow rate. After passing two valves the liquid draining from the high-pressure separator reaches the low-pressure separator (11) where the dissolved gases are separated from the desulfurized oil.

The sulfur content of the feed and of the products was estimated by inductively coupled plasma (ICP). An expanded simulated distillation equipped with a capillary column was used to characterize the boiling-point distribution of the oil. These data were used for estimating liquid properties using standard procedures as published by Ahmed (1989) or in the *API Handbook* (1984). Furthermore, the boiling-point distribution is a simple measure for characterizing the amount of hydrocracking taking place during hydroprocessing (Stangeland, 1974). The content of aromatic C-atoms was determined by ^{13}C-NMR (nuclear magnetic resonance), the Brown–Ladner method (Kägler, 1987) using ^1H-NMR data in combination with the ultimate analysis of carbon and hydrogen, and by the n-d-M method.

Gas-phase samples of the reactor's exit gas stream were analyzed by gas chromatography. A 6 ft (1.8 m) × 2 mm Teflon column packed with Porapak QS was used for the separation of hydrogen sulfide. The gas chromatograph was equipped with a thermal-conductivity detector (TCD) using helium as carrier gas. A second gas chromatograph equipped with a TCD using nitrogen as carrier gas was used for the determination of the hydrogen content in the reactor effluent. The separation was carried out with a 3.1-m × 6-mm column packed with MS 13 X, 80/100 mesh.

After presulfiding, the catalyst passed a state of high activity. The experiments reported here were started after the catalyst activity had reached a constant value, checked periodically by using standard conditions ($p = 10$ MPa, $T = 370$°C, WHSV = 0.90 h^{-1}, $\varphi = 1{,}100$ Nl H_2/kg feed). After steady state had been reached, tested by means of the product oil density and the gas-phase composition, samples were taken and analyzed.

The specifications of the feed used in the experiments are in Table 1.

Reactor Analysis and Kinetic Modeling

As can be seen from Figure 2, the gas/oil ratio has a strong effect on the residual sulfur content of the liquid product.

Table 1. Specifications of the VGO

Characteristic	Dimension
Density at 15.6°C	0.9146 g/cm^3
Density at 50°C	0.8945 g/cm^3
Molecular weight (VPO)	420
Refractive index at 20°C	1.5128
Simulated distillation:	
IBP	245°C
10 vol. %	353°C
30 vol. %	465°C
50 vol. %	524°C
70 vol. %	551°C
90 vol. %	583°C
FBP	617°C
Mean average boiling point	451°C
Ultimate analysis:	
C	85.94 wt. %
H	12.18 wt. %
S	2.00 wt. %
Content of aromatic C-atoms:	
^{1}H-NMR + ultimate analysis	22.4%
n-d-M correlation	23.3%

Hydrodesulfurization is inhibited by hydrogen sulfide that is produced at the sulfided NiMo sites of the bifunctional catalyst and is then transported into the liquid phase. Finally mass transfer of the hydrogen sulfide takes place from the liquid phase into the gas phase. With an increased gas/oil ratio the hydrogen sulfide concentration decreases and as a result the sulfur removal is improved, as shown in Figure 3.

Besides this hydrogen sulfide dilution, an increased gas flow rate can cause an improved mass transfer between the phases or a more uniform liquid distribution. In this case we would expect that the hydrodearomatization might be improved as well as the hydrocracking by an increased gas/oil ratio. As is apparent from Figure 3, variation of the gas/oil ratio does not affect the hydrocracking reactions, but the reduction of the aromatic hydrocarbon content is much better if the H_2S concentration is low.

It should be emphasized that the hydroprocessing reactions take place at two different types of catalytic sites. The hydrotreating reactions, that is, hydrodesulfurization and hydrodearomatization, are catalyzed at the sulfided NiMo sites, whereas the cracking reactions take place at the Al_2O_3 catalyst support. It is obvious that hydrogen sulfide inhibits the hydrotreating reactions by adsorbing at the sulfided NiMo sites. The reactions that are catalyzed by the Al_2O_3 carrier are not influenced by hydrogen sulfide, so that the boiling point curve is not affected by changing the gas/oil ratio.

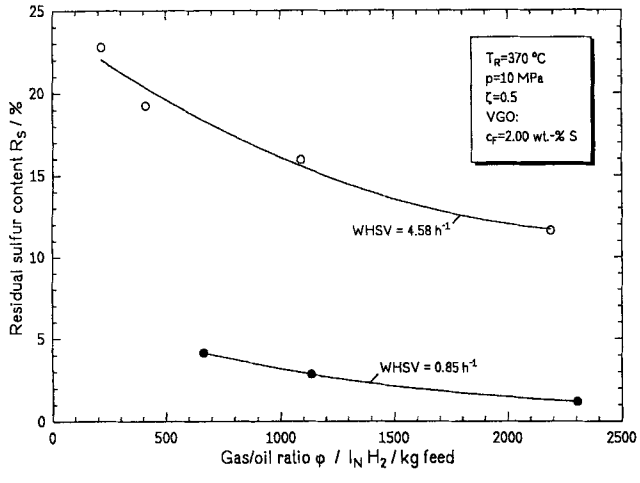

Figure 2. Effect of gas/oil ratio on hydrodesulfurization.

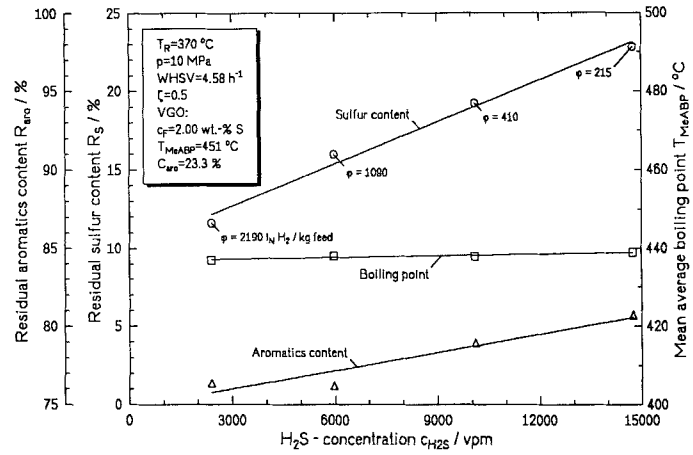

Figure 3. Effect of gas/oil ratio on hydroprocessing.

The concentrations of the compounds in both mobile phases are not constant down through a trickle-bed reactor. Figures 4a and 4b show that the mass transfer and the distribution of hydrogen sulfide in the different phases are very important in modeling hydrotreating reactions. Since these effects are neglected in the pseudohomogeneous plug-flow model, the model is only useful in a small range of parameters. Consequently, the mass conservation equations have to be formulated by taking all three phases into consideration.

Axial dispersion

With respect to the formulation of an adequate reactor simulation we have to analyze whether backmixing can be neglected or not. Considering the flow of gases in fixed beds, Levenspiel (1989) shows that each particle acts like a stirred tank. For the flow of liquids in fixed beds Levenspiel comes to the conclusion that one stirred tank corresponds with 1–4 particles, depending on the Reynolds number. We may assume plug flow in both phases because the catalyst bed contains a large number of particles.

Another criterion, reported by Mears (1971), is useful for the estimation of the minimum bed length L_b we need, so that backmixing effects can be neglected:

$$\frac{L_b}{d_P} > \frac{20\ \text{m}}{Pe_z} \cdot \ln \frac{c_F}{c_P}, \qquad (1)$$

where d_P is the particle diameter, c_F and c_P are the sulfur concentrations in the feed and in the product, respectively. The Peclet number, $u \cdot d_P/D_z$, can be estimated as a function of the Reynolds number, $G \cdot d_P/\mu$. Application of the Mears criterion to the experiments reported here cannot definitely answer the question of whether or not axial dispersion can be neglected. Depending on the correlation used for determin-

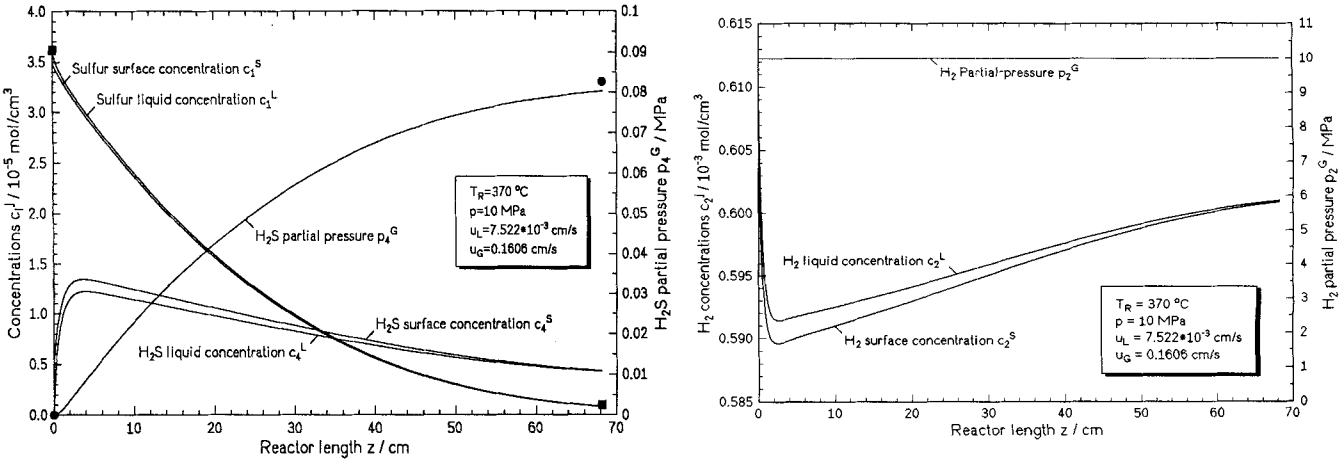

Figure 4. Concentrations down through the reactor.

ing Pe_z, published by Froment and Bischoff (1990) or Baerns et al. (1987), the minimum ratio of L_b/d_P varies between 450 and 3,850, whereas the experimental ratio is 400.

The different results obtained by Levenspiel's and Mears' criteria caused us to carry out some experimental determinations of the residence-time distribution. The residence-time distribution of the gas phase has been measured at 1 MPa and 100°C, displacing hydrogen by nitrogen or vice versa. The actual gas flow rates were adjusted to the values of hydrotreating under the conditions indicated by the black symbols in Figure 2. At the same time a middle distillate fraction had been metered into the reactor. The gas chromatographical analysis of each exit gas stream sample took about 3 minutes.

The residence-time distribution of the liquid phase was measured with respect to the same hydrotreating conditions (Figure 2), using nitrogen as the gaseous compound. In the experiment, vacuum gas oil was displaced by a middle distillate at ambient pressure and 100°C. The liquid samples, taken at the reactor outlet every 3 minutes, were characterized by measuring the refractive index.

Consequently, deviations from plug flow can be neglected for both phases, as predicted by Levenspiel (1989).

Mass-balance equations

By formulating the mass-conservation equations, the following assumptions are made.

1. Gas and liquid velocities are constant across the reactor section.
2. Fluid velocities do not change down through the reactor.
3. There are no radial concentration gradients.
4. The mass transfer can be described by linear mathematical interrelationships.
5. The catalyst activity does not change with time.
6. Vaporization and condensation do not take place.
7. The reactor is operated in steady state.
8. Process conditions are isothermal and of constant pressure.
9. Chemical reactions only take place at the catalyst, and not in the gas or in the liquid phase.
10. Intraparticle mass transfer within the pores of the catalyst may be described by the catalyst effectiveness factor.

In hydrodesulfurization of mineral-oil fractions the following kinds of reaction take place:

$$\text{Generalized:}\quad \nu_1 \cdot A_1\,(\text{Liquid}) + \nu_2 \cdot A_2\,(\text{Gas}) \rightarrow \nu_3 \cdot A_3\,(\text{Liquid}) + \nu_4 \cdot A_4\,(\text{Gas}) \quad (2)$$

$$\text{Mercaptane:}\quad R\text{-SH} + \text{H}_2 \rightarrow \text{RH} + \text{H}_2\text{S} \quad (3)$$

$$\text{Sulfide:}\quad R_2\text{S} + 2\,\text{H}_2 \rightarrow 2\,\text{RH} + \text{H}_2\text{S} \quad (4)$$

$$\text{Disulfide:}\quad (\text{RS}_2) + 3\,\text{H}_2 \rightarrow 2\,\text{RH} + 2\,\text{H}_2\text{S} \quad (5)$$

$$\text{Thiophen:}\quad \text{C}_4\text{H}_4\text{S} + 4\,\text{H}_2 \rightarrow \text{C}_4\text{H}_{10} + \text{H}_2\text{S}. \quad (6)$$

The conversion of petroleum fractions does not allow an exact evaluation of the reactions going on. We will see that the stoichiometric coefficients are a typical characteristic of the feed and can easily be obtained by experiments.

The kinetic modeling is based on the three-film theory as shown in Figure 5. Since no reactions occur in the gas phase, the mass-balance equations for the gaseous compounds are

$$\text{Hydrogen:}\quad \frac{u_G}{R \cdot T} \cdot \frac{dp_2^G}{dz} + k_2^L \cdot a_L \cdot \left(\frac{p_2^G}{\text{H}_2} - c_2^L \right) = 0 \quad (7)$$

$$\text{H}_2\text{S:}\quad \frac{u_G}{R \cdot T} \cdot \frac{dp_4^G}{dz} + k_4^L \cdot a_L \cdot \left(\frac{p_4^G}{\text{H}_4} - c_4^L \right) = 0, \quad (8)$$

where u_G is the superficial velocity of the gas, R is the gas constant; T represents the reactor temperature; p_i^G are the

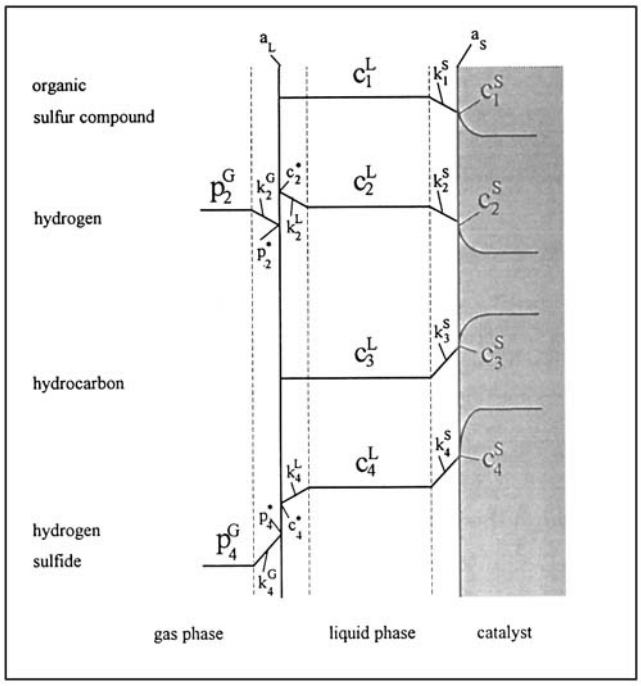

Figure 5. Concentration profiles in a trickle-bed reactor (cf. Hofmann, 1977).

partial pressures of H_2 or H_2S; $k_i^L \cdot a_L$ describes the mass transfer between the gas and the liquid phase; and the liquid-phase concentrations of H_2 and H_2S in equilibrium with the bulk partial pressure are represented by the term p_i^G/H_i. It is assumed that the mass-transfer resistance in the gas film can be neglected.

For the gaseous compounds in the liquid phase the liquid–solid mass transfer, $k_i^S \cdot a_S$, must be taken into consideration:

$$\text{Hydrogen:} \quad u_L \cdot \frac{dc_2^L}{dz} - k_2^L \cdot a_L \cdot \left(\frac{p_2^G}{H_2} - c_2^L \right) + k_2^S \cdot a_S \cdot (c_2^L - c_2^S) = 0 \quad (9)$$

$$\text{H}_2\text{S:} \quad u_L \cdot \frac{dc_4^L}{dz} - k_4^L \cdot a_L \cdot \left(\frac{p_4^G}{H_4} - c_4^L \right) + k_4^S \cdot a_S \cdot (c_4^L - c_4^S) = 0, \quad (10)$$

where u_L is the superficial velocity of the liquid, and c_i^S are the liquid-phase concentrations of H_2 and H_2S at the catalyst surface.

Since the organic sulfur compounds and the liquid hydrocarbons are assumed to be nonvolatile, the mass-balance equations are

$$\text{Organic sulfur:} \quad u_L \cdot \frac{dc_1^L}{dz} + k_1^S \cdot a_S \cdot (c_1^L - c_1^S) = 0 \quad (11)$$

$$\text{Hydrocarbons:} \quad u_L \cdot \frac{dc_3^L}{dz} + k_3^S \cdot a_S \cdot (c_3^L - c_3^S) = 0. \quad (12)$$

The components transported between the liquid phase and the surface of the catalyst are consumed or produced by chemical reaction:

$$\text{Hydrogen:} \quad k_2^S \cdot a_S \cdot (c_2^L - c_2^S) = -\nu_2 \cdot r = -\nu_2 \cdot \rho_b \cdot \zeta \cdot \eta \cdot r_c \quad (13)$$

$$\text{H}_2\text{S:} \quad k_4^S \cdot a_S \cdot (c_4^L - c_4^S) = -\nu_4 \cdot r = -\nu_4 \cdot \rho_b \cdot \zeta \cdot \eta \cdot r_c \quad (14)$$

$$\text{Organic sulfur:} \quad k_1^S \cdot a_S \cdot (c_1^L - c_1^S) = -\nu_1 \cdot r = -\nu_1 \cdot \rho_b \cdot \zeta \cdot \eta \cdot r_c \quad (15)$$

$$\text{Hydrocarbons:} \quad k_3^S \cdot a_S \cdot (c_3^L - c_3^S) = -\nu_3 \cdot r = -\nu_3 \cdot \rho_b \cdot \zeta \cdot \eta \cdot r_c, \quad (16)$$

where ρ_b is the bulk density of the catalyst pellets in the bed, η represents the catalyst effectiveness factor, r_c is the intrinsic rate of reaction per unit mass of the catalyst, and ζ is the ratio of the catalyst bed diluted by inert particles:

$$\zeta = \frac{V_c}{V_c + V_i} \quad (17)$$

where V_c is the volume of active catalyst and V_i is the volume of inert particles.

Since the concentration of hydrocarbons does not change significantly by hydrodesulfurization, Eqs. 12 and 16 will not be taken into further consideration. The five first-order differential equations, Eqs. 7–11, can be solved numerically by a Runge-Kutta method using the following boundary conditions at $z = 0$:

$$c_1^L(z=0) = c_{10}^L \quad (18)$$

$$p_2^G(z=0) = p_{20}^G \quad (19)$$

$$c_2^L(z=0) = c_{20}^L \quad (20)$$

$$p_4^G(z=0) = 0 \quad (21)$$

$$c_4^L(z=0) = 0. \quad (22)$$

Assuming the organic sulfur compound has the same molecular weight as the whole sample, its concentration can be estimated by using the weight fraction w_1, as determined by ICP:

$$c_1^L = \frac{\rho_1}{M_1} \cdot w_1. \quad (23)$$

The density ρ_1 of the oil at process conditions can be determined by the Standing–Katz correlation, as presented in Ahmed (1989). In deviating from the SI system we give the equation with the original units:

$$\rho(p,T) = \rho_0 + \Delta\rho_p - \Delta\rho_T, \quad (24)$$

where ρ_0 represents the density at standard conditions

(15.6°C; 101.3 kPa) in lb/ft^3. The pressure dependence can be calculated by

$$\Delta\rho_p = [0.167 + 16.181 \cdot 10^{-0.0425 \cdot \rho_0}] \cdot \left[\frac{p}{1{,}000}\right] - 0.01 \cdot [0.299 + 263 \cdot 10^{-0.0603 \cdot \rho_0}] \cdot \left[\frac{p}{1{,}000}\right]^2, \quad (25)$$

where p is the pressure in psia. Since the density drops with rising temperature, a temperature correction with the temperature T in °R is given:

$$\Delta\rho_T = \left[0.0133 + 152.4 \cdot (\rho_0 + \Delta\rho_p)^{-2.45}\right] \cdot [T - 520] - [8.1 \cdot 10^{-6} - 0.0622 \cdot 10^{-0.764 \cdot (\rho_0 + \Delta\rho_p)}] \cdot [T - 520]^2. \quad (26)$$

The mass-balance equations are based on the assumption that the gas–liquid equilibrium can be described by Henry's law. The Henry coefficient H_i can be obtained from solubility coefficients λ_i:

$$H_i = \frac{v_N}{\lambda_i \cdot \rho_L} \quad (27)$$

where v_N is the molar gas volume at standard conditions and ρ_L represents the density of the liquid under process conditions. Taking data from the literature, we derived the following correlations for the solubility of hydrogen and hydrogen sulfide in hydrocarbon mixtures:

$$\text{Hydrogen:} \quad \lambda_2 = a_0 + a_1 \cdot T + a_2 \cdot \frac{T}{\rho_{20}} + a_3 \cdot T^2 + a_4 \cdot \frac{1}{\rho_{20}^2} \quad (28)$$

with the constants

$$a_0 = -0.559729 \qquad a_3 = 1.94593 \cdot 10^{-6}$$
$$a_1 = -0.42947 \times 10^{-3} \qquad a_4 = 0.835783$$
$$a_2 = 3.07539 \times 10^{-3}$$

where T is the temperature in °C, ρ_{20} represents the density at 20°C in g/cm^3, and the hydrogen solubility is given in (Nl H_2)/[(kg oil)·(MPa)]. We found the solubility of hydrogen sulfide in mineral-oil fractions to be

$$\lambda_4 = \exp(3.3670 - 0.008470 \cdot T). \quad (29)$$

External mass transfer

The gas–liquid mass-transfer coefficient is a function of the liquid superficial mass-flow velocity G_L. For its determination we use the correlation published by Goto and Smith (1975):

$$\frac{k_i^L \cdot a_L}{D_i^L} = \alpha_1 \cdot \left(\frac{G_L}{\mu_L}\right)^{\alpha_2} \cdot \left(\frac{\mu_L}{\rho_L \cdot D_i^L}\right)^{1/2}, \quad (30)$$

where the term $k_i^L \cdot a_L$ represents the mass transfer, and ρ_L is the density of the liquid as determined by Eqs. 24–26. The coefficients α_1 and α_2 are a function of the particle diameter. For the pellets used in this article, $d_P = 1.72$ mm, we get $\alpha_2 = 0.4$ and $\alpha_1 = 7\ (\text{cm})^{-1.6}$.

The dependence of dynamic liquid viscosity μ_L on temperature may be described by the Vogel equation, as published by Reid et al. (1987). The disadvantage of using this correlation is that it cannot be applied to a hydrocarbon mixture of unknown composition until three parameters have been determined experimentally. Using the density of the oil as a parameter, Glaso's correlation, as published in Ahmed (1989), shows good agreement with the measured values. In terms of API gravity this equation gives the viscosity in mPa·s:

$$\mu = 3.141 \cdot 10^{10} \cdot (T - 460)^{-3.444} \cdot [\log_{10}(API)]^a, \quad (31)$$

where

$$a = 10.313 \cdot [\log_{10}(T - 460)] - 36.447, \quad (32)$$

with temperature T in °R. We can take into account the small dependence of liquid viscosity on pressure within the range of interest by using the procedure published in the *API Handbook* (1984).

It is necessary to know the molecular diffusivity D_i^L of solute i in the liquid in order to use Eq. 30 to determine the gas–liquid mass-transfer coefficients. Assuming infinite dilution, the diffusivity can be estimated by a Tyn-Calus correlation, as published by Reid et al. (1987):

$$D_i^L = 8.93 \cdot 10^{-8} \cdot \frac{v_L^{0.267}}{v_i^{0.433}} \cdot \frac{T}{\mu_L}, \quad (33)$$

where T is the temperature in K and μ_L represents the viscosity of the solvent in mPa·s. By using Eq. 33 we obtain the diffusivity in cm^2/s. The molar volume of solute, v_i, or liquid solvent, v_L, at its normal boiling temperature can be estimated as published in Perry and Green (1984):

$$v = 0.285 \cdot v_c^{1.048}. \quad (34)$$

The measurement unit of the molar volume is cm^3/mol. The critical specific volume v_c of the gaseous compounds H_2 and H_2S is tabulated in Reid et al. (1987), whereas for the liquid components this characteristic can be obtained by using the Riazi-Daubert correlation (Ahmed, 1989):

$$v_c^m = 7.5214 \cdot 10^{-3} \cdot T_{\text{MeABP}}^{0.2896} \cdot d_{15.6}^{-0.7666}, \quad (35)$$

where v_c^m is the critical specific volume in ft^3/lb, T_{MeABP} represents the mean average boiling point in °R and $d_{15.6}$ is the specific gravity at 15.6°C. The transformation of v_c^m to v_c can be carried out by multiplication with the molecular weight M.

Because of the complex composition of hydrocarbon mixtures, some assumptions are necessary before using Eq. 33. We consider the organic sulfur compound to have the same density, average boiling point, and molecular weight as the

whole liquid sample. In this case the molar volume of the medium sulfur compound is equal to that of the liquid solvent, $v_1 = v_L$. The diffusivity decreases because the viscosity rises with increasing pressure.

The liquid–solid mass transfer in the low interaction regime can be estimated by the van Krevelen–Krekels equation (Froment and Bischoff, 1990):

$$\frac{k_i^S}{D_i^L \cdot a_S} = 1.8 \cdot \left(\frac{G_L}{a_S \cdot \mu_L}\right)^{1/2} \cdot \left(\frac{\mu_L}{\rho_L \cdot D_i^L}\right)^{1/3}, \qquad (36)$$

where a_S is the specific surface area of the packing:

$$a_S = \frac{6}{d_P} \cdot (1 - \epsilon), \qquad (37)$$

where d_P is the equivalent particle diameter and ϵ is the void fraction of the catalyst bed.

Using their new criterion, Satterfield et al. (1969) show that with regard to the hydrodesulfurization of middle distillates in industrial plants, mass-transfer phenomena can be neglected. If the inequality is true, mass transfer cannot be neglected:

$$\frac{10 \cdot d_P}{3 \cdot c_i^L} \cdot (-\nu_i \cdot r) > k_i^S, \qquad (38)$$

where
d_P = particle diameter, cm
c_i^L = concentration in the liquid phase, mol/cm^3
r = reaction rate, mol/[(cm^3 catalyst)·s]
k_i^S = mass-transfer coefficient, cm/s

By using the criterion for hydrodesulfurization of vacuum gas oil (VGO) in an industrial trickle-bed reactor, as characterized in Table 1, we come to the same conclusion as Satterfield et al. (1969) that mass transfer does not play an important role. Table 2 shows typical process conditions of our pilot plant and of an industrial hydrotreater, as well as a comparison of the mass-transfer data. Since the liquid superficial mass-flow velocity in a pilot plant reactor with a diluted catalyst bed is about 70 times smaller than in an industrial plant, the gas–liquid and liquid–solid mass transfer is much better in the latter one. In pilot plants the left and the right sides of Satterfield's criterion (Eq. 38) are of the same order of magnitude. Consequently, the assumption that mass transfer in pilot plant reactors could be neglected is very doubtful.

Table 2. Mass Transfer in Trickle-Bed Reactors

	Pilot Plant	Industrial Plant
Pres. p, MPa	10	
Temp. T, °C	370	
WHSV, h^{-1}	0.85	
Mass flow G_L, g/(cm^2·s)	0.00572	0.4
Diffusivities, cm^2/s		
Org. sulfur comp. (D_1^L)	3.25×10^{-5}	
Hydrogen (D_2^L)	1.33×10^{-4}	
Hydrogen sulfide (D_4^L)	1.10×10^{-4}	
Gas–liquid mass transfer, s^{-1}		
Hydrogen ($k_2^L \cdot a_L$)	7.05×10^{-3}	3.86×10^{-2}
Hydrogen sulfide ($k_4^L \cdot a_L$)	6.42×10^{-3}	3.51×10^{-2}
Liquid–solid mass transfer, s^{-1}		
Organic sulfur comp. ($k_1^S \cdot a_S$)	2.76×10^{-2}	0.231
Hydrogen ($k_2^S \cdot a_S$)	7.06×10^{-2}	0.590
Hydrogen sulfide ($k_4^S \cdot a_S$)	6.22×10^{-2}	0.520
Reaction rate $\nu_2 \cdot r$, mol/(cm^3·s)	2.53×10^{-6}	
H_2 mass transfer k_2^S, cm/s	3.88×10^{-3}	3.24×10^{-2}
Left side of Eq. 38, cm/s	2.38×10^{-3}	

Rate of chemical reaction and intrapellet mass transfer

Since hydrodesulfurization reactions at the usual process conditions are irreversible (Girgis and Gates, 1991; Vrinat, 1983), reverse reactions need not be considered.

Assuming the sulfur content of the oil and the concentration of hydrogen to have a positive effect, and hydrogen sulfide to adsorb at the active catalyst sites, the following kinetic equation of the Langmuir–Hinshelwood type is used:

$$r_C = k_{\text{app}} \cdot \frac{(c_1^S)^{m_1} \cdot (c_2^S)^{m_2}}{(1 + K_4 \cdot c_4^S)^2}, \qquad (39)$$

where the rate of reaction per unit mass of the catalyst is correlated with the concentrations c_i^S at the outer catalyst surface; m_1 and m_2 represent the reaction order concerning the sulfur compound and hydrogen, respectively; k_{app} is the apparent rate constant, as discussed below; and the adsorption-equilibrium constant of hydrogen sulfide at the catalyst surface is represented by K_4.

It has often been observed that the rate of chemical reaction decreases with increasing particle size. Especially in the hydrotreating of high-boiling mineral-oil fractions, a great intrapellet mass-transfer resistance must be expected. In the literature effectiveness factors in the range of $\eta = 0.0057$–1 are mentioned (Li et al., 1995; Scamangas and Marangozis, 1982; Weiss et al., 1987).

In the calculations described below we assumed that the catalyst effectiveness factor is constant down through the reactor. Since the experiments reported in this article are carried out using a single catalyst charge, the value of the catalyst effectiveness factor is included in the chemical reaction rate constant. The validity of assuming a constant effectiveness factor in the field of hydroprocessing is confirmed by the good agreement with the experimental results. This simplification makes it much easier to solve the system of equations than it would be if the concentration profile inside the catalyst were included, as recently noted by Froment et al. (1994).

Reactor Performance and Simulation

The three-phase reactor model contains a number of parameters. Most of these, the properties of gases and liquids, solubilities, diffusivities, and mass-transfer coefficients, can be calculated by using the correlations given earlier. The rate constant, order of reaction, and adsorption equilibrium constant are the result of experimental determination.

The stoichiometric coefficients of the overall hydrodesulfurization reaction as a characteristic of the feed have to be estimated experimentally because information about the chemical composition of high-boiling petroleum fractions is lacking. Referring to Eqs. 2 to 6, the stoichiometric coeffi-

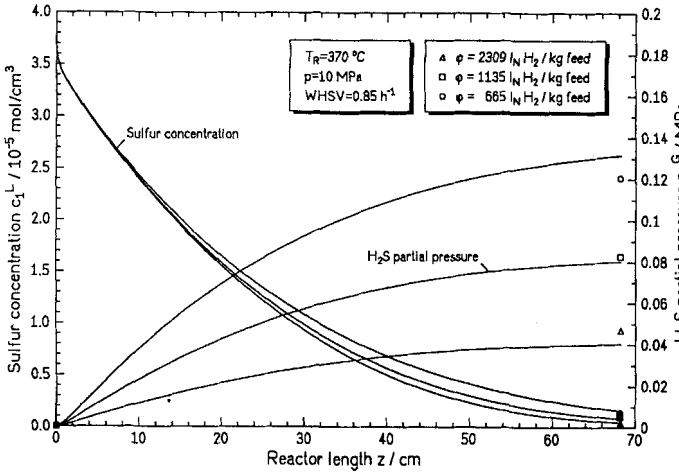

Figure 6. Sulfur and H_2S concentrations down through the reactor.

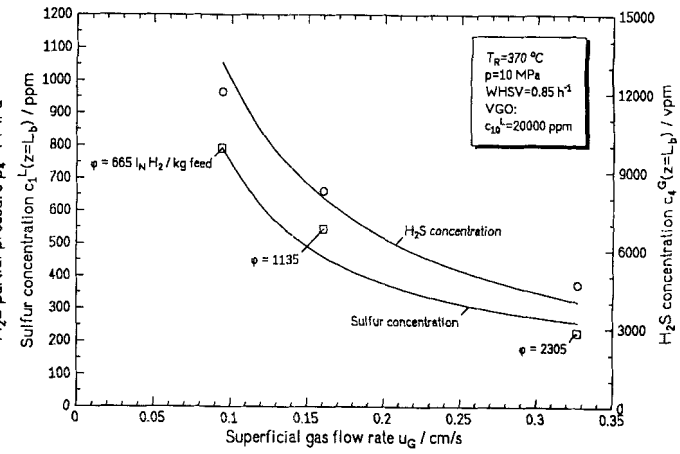

Figure 8. Effect of gas/oil ratio at low liquid flow rate.

cient of the organic sulfur compound is $\nu_1 = -1$. Using the measured concentrations of hydrogen sulfide at the reactor inlet and reactor outlet, the stoichiometric coefficient ν_4 can be easily estimated. Since hydrogen is used in excess, its stoichiometric coefficient ν_2 does not influence the simulation as strongly as ν_4. Using the feed as specified in Table 1, the stoichiometric coefficient of hydrogen sulfide was estimated to be $\nu_4 = 9$. This value was calculated by using a univariable method (Hoffmann and Hofmann, 1971) from the data shown in Figure 6. The stoichiometric coefficient of hydrogen was set to $\nu_2 = -15$.

Orders of reaction are $m_1 = 1$ and $m_2 = 0.45$. The value of m_2 appears to be due to a dissociation of H_2 at the catalyst sites, where the theoretical value would be $m_2 = 0.5$. These parameters and the adsorption-equilibrium constant of hydrogen sulfide at the catalyst, $K_4 = 70{,}000$ cm^3/mol, were estimated as well as the reaction rate constant by applying a univariable method, using the data shown in Figures 7, 8, and 9.

The simulated concentration profiles in the reactor, based on the parameters given earlier, are illustrated in Figures 4a and 4b.

Space velocity and contacting effectiveness

A comparison of experimental data, obtained by adjusting space velocities in the range of WHSV = 0.85–4.58 h^{-1}, with the reactor simulation shows that the apparent rate constant k_{app} increases with WHSV. This effect can be correlated with the wetting efficiency, defined as the ratio of the apparent rate constant k_{app} and the intrinsic rate constant k_{in}:

$$f_w = \frac{k_{app}}{k_{in}} \leq 1. \tag{40}$$

The trickling-flow regime is subdivided into a complete and a partial wetting region, depending on the liquid flow rate (Ng, 1986; Ng and Chu, 1987). Because of the small superficial mass-flow velocities in pilot trickle-bed reactors, the wetting efficiency is in the range $f_w = 0.12$–0.6 (Satterfield, 1975; Gates et al., 1979). The wetting efficiency of industrial reactors can be expected to be $f_w = 0.7$–1.0.

There are a number of correlations in the literature that predict the wetting efficiency of packing materials. Since the wetting efficiency is a function of the initial liquid distribution, the geometry of the packing and of the catalyst, and the

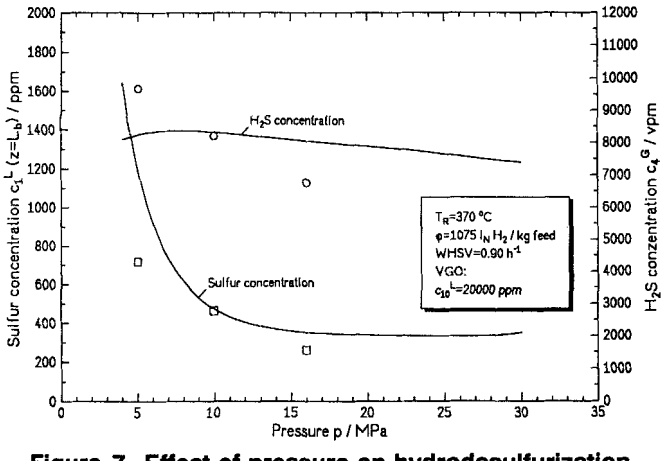

Figure 7. Effect of pressure on hydrodesulfurization.

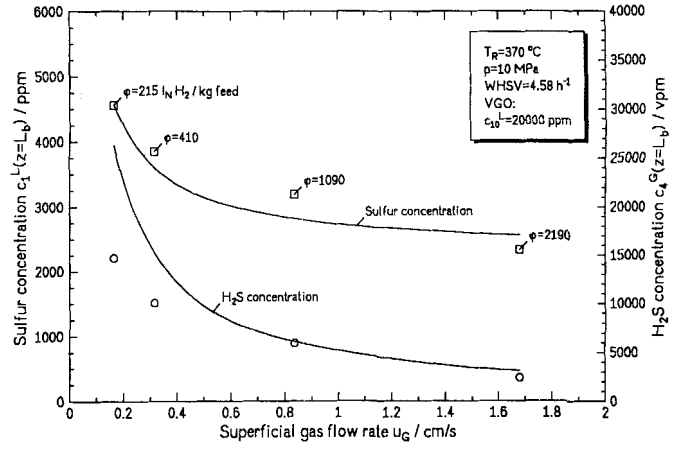

Figure 9. Influence of gas/oil ratio at elevated liquid flow rate.

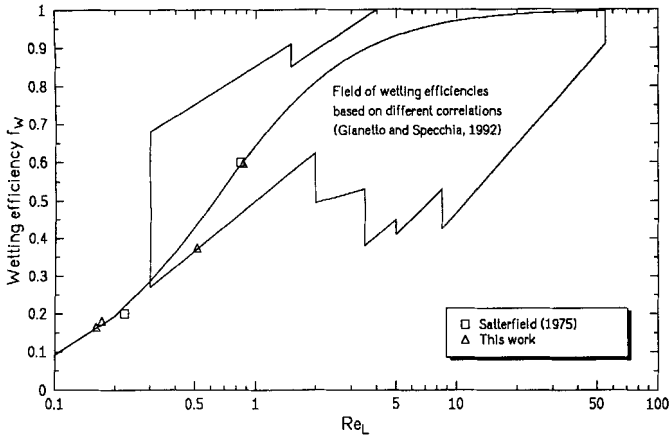

Figure 10. Wetting efficiency in a trickle-bed reactor.

mass flow throughout the reactor, the predicted values are scattered over a wide range, as shown in Figure 10. Figure 10 is based on an article by Gianetto and Specchia (1992).

Using an empirical correlation, as recommended by Satterfield (1975), the measured values of the apparent rate constant as a function of the superficial mass-flow velocity G_L in kg/(m^2·s) can be described very well, as shown in Figure 10:

$$\frac{1}{k_{app}} - \frac{1}{k_{in}} = \frac{A}{G_L^B}, \tag{41}$$

with the intrinsic rate constant $k_{in} = 0.67$ (cm^3/(g·s))·(cm^3/mol)$^{0.45}$ and the constants $A = 0.21$ and $B = 1.40$.

It should be noted that the conversion in trickle-bed reactors depends strongly on the wetting efficiency. The deviation of the measured sulfur concentrations from the reactor simulation curve, as shown in Figure 11, is due to the reasonable correspondence of the experimental data, which are expressed by Eqs. 40 and 41 and illustrated in Figure 10. A small overestimate of the wetting efficiency by the theoretical curve in Figure 10 allows the reactor model to calculate a sulfur conversion that is too high (Figure 11).

The strong influence of the wetting efficiency on the conversion is due to small catalyst effectiveness factors, as observed in hydroprocessing heavy fractions. In the case of partial wetting we have to distinguish between an incomplete-contact reactor scale and an incomplete-contact particle scale (Mills and Dudukovic, 1979). The former describes a situation where parts of the catalyst bed are completely dry, so that the total reactor efficiency is proportional to the wetting efficiency. If the catalyst particles are touched by the liquid without wetting the whole surface, we call it incomplete-contact particle scale. Because of capillary forces, we assume the pellet to be completely liquid-filled if it comes in contact with the liquid. In pilot plant reactors we consider the incomplete-contact particle scale. In the case of large Thiele modulus, that is, very fast reaction, the total catalyst effectiveness is strongly affected by the external wetting efficiency. This is because the liquid reactant cannot get into the catalyst rapidly enough if the wetting efficiency is small. The reaction takes place only in a thin shell near the wetted catalyst surface. Considering a slow reaction, where the intraparticle mass transfer can be neglected, that is, small Thiele modulus, the problem of liquid-reactant depletion is much less, and therefore the total catalyst effectiveness is relatively unaffected by external wetting efficiency (Mills and Dudukovic, 1979; Harold and Ng, 1987).

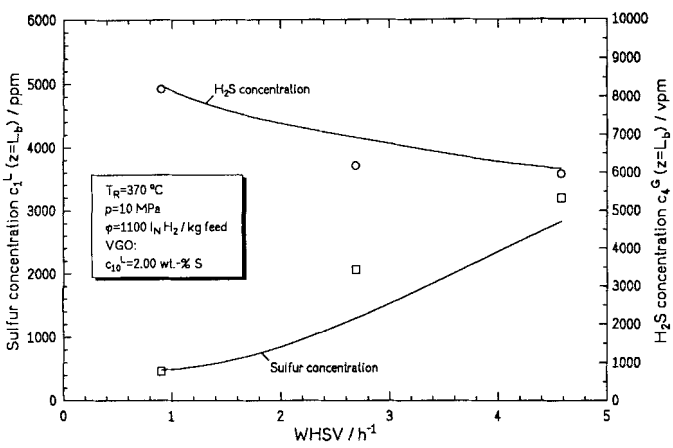

Figure 11. Variation of space velocity on hydrodesulfurization.

Effect of pressure

Since the order of the hydrogen concentration reaction at the surface of the catalyst is $m_2 = 0.45$, the conversion of the organic sulfur compounds increases with pressure. Figure 7 shows that the effect of pressure decreases with increasing pressure. This influence can be neglected above 12 MPa. Since the viscosity of the oil increases with pressure, diffusivity and mass-transfer coefficients decrease. Therefore at high pressure a diminution of the conversion may be observed.

The produced quantity of hydrogen sulfide generally goes up as the conversion of the organic sulfur compounds increases. As we can see in Figure 7, the concentration of H_2S in the gas phase goes down, because the solubility of gases in liquids increases with rising partial pressure. A deviation exists between the measured H_2S concentration in the gas phase and the values that are predicted by our model, represented by the curve in Figure 7. The calculation of the gas–liquid equilibria by Henry's law may be the source of this difference. Recall that Henry coefficients generally are not independent of pressure and that the proper application of Henry's law is restricted to small concentrations of the solute.

Effect of gas/oil ratio

As mentioned earlier, the pseudohomogeneous plug-flow model should not be used for hydrodesulfurization in trickle-bed reactors, unless a crude approximation is required. The three-phase reactor model is in good agreement with the experimental results. As we can see in Figure 6, the partial pressure of hydrogen sulfide increases down through the reactor, and the sulfur conversion can be improved by increasing the gas/oil ratio. In the literature experiments have mostly been carried out at gas/oil ratios of $\varphi = 300$–900 (Nl H_2)/(kg feed), a range where the conversion is strongly inhibited by hydrogen sulfide (Figure 8).

With the elevated mass flow velocity of the liquid phase, the apparent rate constant increases. This increased rate con-

stant can be estimated using Eq. 41. Based on this value, Figure 9 shows that, within a wide range of gas/oil ratios, the simulation agrees reasonably well with the experimental results.

Effect of temperature

The following parameters of the reactor model are influenced by temperature:

1. Velocities of the gas and of the liquid flow
2. Diffusivities of the compounds
3. Mass transfer at the gas–liquid and at the liquid–solid interfaces
4. Henry's coefficients of hydrogen and hydrogen sulfide in the oil
5. Viscosities of the compounds
6. Densities of the compounds.

The temperature dependence of these parameters can be estimated by the correlations given earlier. But the effect of temperature on the rate constant and on the adsorption equilibrium constant of hydrogen sulfide at the catalyst has to be experimentally estimated.

The influence of temperature on the adsorption-equilibrium constant can be be described by the van't Hoff equation:

$$K_4(T) = K_0 \cdot \exp\left(\frac{\Delta H_{ads}}{R \cdot T}\right). \qquad (42)$$

The enthalpy of adsorption of hydrogen sulfide on an alumina-supported CoMo catalyst has been estimated to be $\Delta H_{ads} = 2{,}761$ J/mol in a temperature range of $T = 533$–644 K (Frye and Mosby, 1967). If the temperature rises from 370 to 390°C, the adsorption equilibrium constant decreases by 1.6%. In comparison with the effect of temperature on the rate constant, the temperature dependence of the equilibrium constant can be neglected.

Experiments have been carried out at temperatures between 350 and 390°C. Using the Arrhenius equation,

$$k = k_0 \cdot \exp\left(-\frac{E_A}{R \cdot T}\right), \qquad (43)$$

the activation energy could be estimated to be $E_A = 72.5$ kJ/mol, and the frequency factor is $k_0 = 0.545 \cdot 10^6$ $(cm^3/(g \cdot s)) \cdot (cm^3/mol)^{0.45}$. The vacuum gas oil used in these experiments was specified by a higher sulfur content, molecular weight and mean average boiling point than the vacuum gas oil used in the other experiments reported here. Using the parameter estimation methods previously described, the simulation is in good agreement with the experimental data (Figure 12). The stoichiometric coefficient of hydrogen sulfide, which is a characteristic of the oil, is $\nu_4 = 10$.

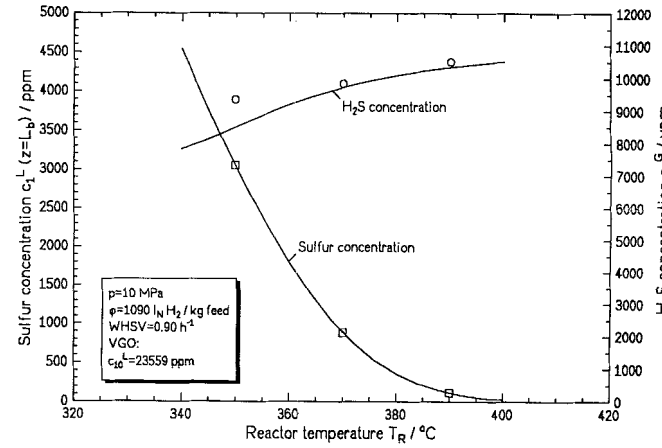

Figure 12. Temperature dependence during hydrodesulfurization.

Discussion and Conclusions

Since hydrodesulfurization is strongly limited by hydrogen sulfide, the chemical reaction rate is expressed by a Langmuir–Hinshelwood formulation in terms of catalyst surface concentrations. The hydrogen sulfide concentration down through the reactor decreases with increasing gas/oil ratio, so that the sulfur conversion becomes much better. This fact cannot be described by a homogeneous plug-flow model, and consequently, a three-phase reactor model is presented here.

The model contains mass-transport phenomena at the gas–liquid and at the liquid–solid interface. In the literature a number of correlations for predicting mass-transfer coefficients are presented. These have been developed in nonreacting systems, and mostly at ambient pressure and temperature. For the estimation of mass-transfer coefficients the knowledge of density, viscosity, and molecular diffusivity under process conditions is essential. Since high-boiling petroleum fractions become unstable at temperatures above 350°C, the estimation of these properties may include some uncertainty. Nevertheless, the mathematical simulation shows reasonably good agreement with the experimental results.

A scale-up of pilot plant data to an industrial trickle-bed reactor can yield some miscalculation, because the superficial mass-flow velocity in the large-scale reactor is much higher than in pilot plants. Since the contact effectiveness strongly depends on the mass-flow velocity, the wetting efficiency in pilot plant reactors is about $f_w = 0.15$–0.6, whereas a complete catalyst wetting can be expected in industrial plants. Because of its large diameter in a commercial reactor, an incomplete wetting also may occur if the liquid distributor is unsuitable.

In hydrotreating heavy feed, very small catalyst effectiveness factors have been observed, which means that the reactions take place only in a small sphere near the outer surface area of the catalyst. In this case, the chemical reaction rate strongly depends on the wetting efficiency. Contact effectiveness factors, estimated by a number of correlations, are scattered over a wide range. Since the wetting efficiency depends on the geometrical data of the reactor system, properties of the feed, process conditions, and reactor start-up, this insufficiency is explainable.

Of course, it can be advantageous to dilute the catalyst bed with fine inert particles. At present, however, a quantitative method for determining catalyst wetting efficiencies in diluted beds does not exist.

Acknowledgment

The work was financially supported by the German government

and Veba Oel AG. We would like to thank Prof. Dr. D. Severin and Dr. I. Rahimian, Institut für Erdöl- und Erdgasforschung, for performing a number of analytical procedures.

Notation

a_L = specific gas–liquid interface, cm^{-1}
K_0 = adsorption-equilibrium constant at infinite temperature, cm^3/mol
R_{aro} = residual aromatics content
R_S = residual sulfur content
z = axial coordinate in reactor, cm

Subscripts and superscripts

c = critical
L = liquid
S = solid
3 = hydrocarbon

Literature Cited

Ahmed, T., *Hydrocarbon Phase Behavior*, Gulf Publishing, Houston (1989).
API, *Technical Data Book—Petroleum Refining*, Amer. Pet. Inst. (1984).
Baerns, M., H. Hofmann, and A. Renken, *Chemische Reaktionstechnik*, Georg Thieme Verlag, Stuttgart (1987).
Bondi, A., "Handling Kinetics from Trickle-phase Reactors," *Chem. Tech.*, 185 (1971).
Froment, G. F., and K. B. Bischoff, *Chemical Reactor Analysis and Design*, 2nd ed., Wiley, New York (1990).
Froment, G. F., G. A. Depauw, and V. Vanrysselberghe, "Kinetic Modeling and Reactor Simulation in Hydrodesulfurization of Oil Fractions," *Ind. Eng. Chem. Res.*, **33**, 2975 (1994).
Frye, C. G., and J. F. Mosby, "Kinetics of Hydrodesulfurization," *Chem. Eng. Prog.*, **63**, 66 (Sept., 1967).
Gates, B. C., J. R. Katzer, and G. C. A. Schuit, *Chemistry of Catalytic Processes*, McGraw-Hill, New York (1979).
Gianetto, A., and V. Specchia, "Trickle-bed Reactors: State of Art and Perspectives," *Chem. Eng. Sci.*, **47**, 3197 (1992).
Goto, S., and J. M. Smith, "Trickle-bed Reactor Performance: I. Holdup and Mass Transfer Effects," *AIChE J.*, **21**, 706 (1975).
Harold, M. P., and K. M. Ng, "Effectiveness Enhancement and Reactant Depletion in a Partially Wetted Catalyst," *AIChE J.*, **33**, 1448 (1987).
Henry, H. C., and J. B. Gilbert, "Scale Up of Pilot Plant Data for Catalytic Hydroprocessing," *Ind. Eng. Chem. Process Des. Dev.*, **12**, 328 (1973).
Hoffmann, U., and H. Hofmann, *Einführung in die Optimierung*, Verlag Chemie, Weinheim (1971).
Hofmann, H., "Hydrodynamics, Transport Phenomena, and Mathematical Models in Trickle-Bed Reactors," *Int. Chem. Eng.*, **17**, 19 (1977).
Kägler, S. H., ed., *Neue Mineralölanalyse: Band 1: Spektroskopie*, 2nd ed., Hüthig, Heidelberg (1987).
Korsten, H., and U. Hoffmann, "Hydrotreating of Vacuum Gas Oil in a New High-Pressure Pilot Plant," *Erdöl Erdgas Kohle*, **111**, 468 (1995).
Levenspiel, O., *The Chemical Reactor Omnibook*, Oregon State Univ., Corvallis (1989).
Li, C., Y.-W. Chen, and M.-C. Tsai, "Highly Restrictive Diffusion under Hydrotreating Reactions of Heavy Residue Oils," *Ind. Eng. Chem. Res.*, **34**, 898 (1995).
Mears, D. E., "The Role of Axial Dispersion in Trickle-Flow Laboratory Reactors," *Chem. Eng. Sci.*, **26**, 1361 (1971).
Mears, D. E., "The Role of Liquid Holdup and Effective Wetting in the Performance of Trickle-Bed Reactors," *Advances in Chemistry*, ACS Ser. No. 133, 218 (1974).
Mills, P. L., and M. P. Dudukovic, "A Dual-Series Solution for the Effectiveness Factor of Partially Wetted Catalysts in Trickle-Bed Reactors," *Ind. Eng. Chem. Fundam.*, **18**, 139 (1979).
Ng, K. M., "A Model for Flow Regime Transitions in Cocurrent Down-Flow Trickle-Bed Reactors," *AIChE J.*, **32**, 115 (1986).
Ng, K. M., and C. F. Chu, "Trickle-Bed Reactors," *Chem. Eng. Prog.*, **83**, 55 (Nov. 1987).
Papayannakos, N., and J. Marangozis, "Kinetics of Catalytic Hydrodesulfurization of a Petroleum Residue in a Batch-recycle Trickle Bed Reactor," *Chem. Eng. Sci.*, **39**, 1051 (1984).
Paraskos, J. A., J. A. Frayer, and Y. T. Shah, "Effect of Holdup Incomplete Catalyst Wetting and Backmixing during Hydroprocessing in Trickle Bed Reactors," *Ind. Eng. Chem. Process Des. Dev.*, **14**, 315 (1975).
Parijs, I. A. van, and G. F. Froment, "Kinetics of Hydrodesulfurization on a $CoMo/\gamma\text{-}Al_2O_3$ Catalyst: 1. Kinetics of the Hydrogenolysis of Thiophene," *Ind. Eng. Chem. Prod. Res. Dev.*, **25**, 431 (1986).
Parijs, I. A. van, L. H. Hosten, and G. F. Froment, "Kinetics of Hydrodesulfurization on a $CoMo/\gamma\text{-}Al_2O_3$ Catalyst: 2. Kinetics of the Hydrogenolysis of Benzothiophene," *Ind. Eng. Chem. Prod. Res. Dev.*, **25**, 437 (1986).
Perry, R. H., and D. Green, eds., *Perry's Chemical Engineers' Handbook*, 6th ed., McGraw-Hill, New York (1984).
Reid, R. C., J. M. Prausnitz, and B. E. Poling, *The Properties of Gases & Liquids*, 4th ed., McGraw-Hill, New York (1987).
Satterfield, C. N., A. A Pelossof, and T. K. Sherwood, "Mass Transfer Limitations in a Trickle-Bed Reactor," *AIChE J.*, **15**, 226 (1969).
Satterfield, C. N., "Trickle-Bed Reactors," *AIChE J.*, **21**, 209 (1975).
Scamangas, A., and N. Marangozis, "Catalytic Hydrodesulfurization of a Petroleum Residue," *Chem. Eng. Sci.*, **37**, 812 (1982).
Stangeland, B. E., "A Kinetic Model for the Prediction of Hydrocracker Yields," *Ind. Eng. Chem. Process Des. Dev.*, **13**, 71 (1974).
Stephan, R., G. Emig, and H. Hofmann, "On the Kinetics of Hydrodesulfurization of Gas Oil," *Chem. Eng. Process.*, **19**, 303 (1985).
Vrinat, M. L., "The Kinetics of Hydrodesulfurization Processes—A Review," *Appl. Catal.*, **6**, 137 (1983).
Weiss, S., W. Berghoff, E. Grahn, G. Gruhn, M. Guesewell, W. Ploetner, H. Robel, and M. Schubert, eds., *Verfahrenstechnische Berechmungsmethoden: Teil 5. Chemische Reaktoren*, Verlag Chemie, Weinheim (1987).

Manuscript received Dec. 27, 1994, and revision received Aug. 16, 1995.